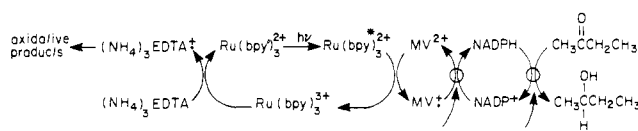


**Figure 1.** Rate of 2-butanol formation at different illumination time intervals. Initial  $(\text{NH}_4)_3\text{EDTA}$  concentration  $2 \times 10^{-2}$  M. (a) Addition of  $(\text{NH}_4)_3\text{EDTA}$ ,  $2 \times 10^{-2}$  M, (b) addition of  $(\text{NH}_4)_3\text{EDTA}$ ,  $1.7 \times 10^{-2}$  M, (c) addition of  $(\text{NH}_4)_3\text{EDTA}$ ,  $1.7 \times 10^{-2}$  M.



**Figure 2.** Cyclic scheme for the photosensitized reduction of 2-butanone by  $(\text{NH}_4)_3\text{EDTA}$ .

**Table I.** Turnover Numbers (TN) of Components Involved in the Photosensitized Reduction of 2-Butanone

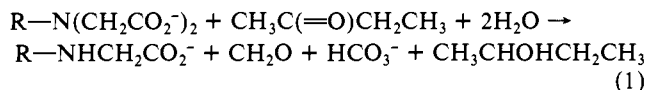
	$\text{Ru}(\text{bpy})_3^{2+}$	$\text{MV}^{2+}$	$\text{FDR}^a$	$\text{NADP}^+$	$\text{ALDH}^b$
TN	530	40	24 000	40	6000

<sup>a</sup>FW  $\approx$  40 000; cf.: Shin, M. *Methods Enzymol.* **1971**, *23*, 441.  
<sup>b</sup>FW  $\approx$  40 000.<sup>9</sup>

and their different turnover numbers after 40 h of illumination are summarized in Table I.

The different steps involved in the photoinduced reduction of 2-butanone have been confirmed by separate experiments. Illumination of the aqueous system that includes only the sensitizer,  $(\text{NH}_4)_3\text{EDTA}$ ,  $\text{MV}^{2+}$ ,  $\text{NADP}^+$  and the enzyme ferredoxin reductase, results in the formation of NADPH (followed spectroscopically at  $\lambda = 340$  nm). When either  $\text{MV}^{2+}$  or ferredoxin reductase are excluded from the system no photosensitized formation of NADPH is observed. These results imply that  $\text{MV}^+$  formed upon illumination mediates the reduction of  $\text{NADP}^+$  to NADPH in the presence of the enzyme.<sup>11</sup> Introduction of 2-butanone to the photochemically produced NADPH does not lead to the disappearance of NADPH, and no alcohol is formed. Yet, upon introduction of the enzyme alcohol dehydrogenase the NADPH disappears and 2-butanol is observed as product. These facts confirm that NADPH mediates the reduction of 2-butanone in the presence of the second enzyme.<sup>9</sup> In view of these results we suggest the scheme outlined in Figure 2 as the cyclic photoinduced process leading to the reduction of 2-butanone. This cycle involves a photosystem that produces  $\text{MV}^+$  and two subunits of enzyme-catalyzed reactions. In the first unit NADPH is formed in a process catalyzed by ferredoxin-NADP<sup>+</sup> reductase. The subsequent unit utilizes NADPH in the reduction of 2-butanone in the presence of alcohol dehydrogenase.

The net reaction accomplished in this system corresponds to the reduction of 2-butanone by EDTA (eq 1).<sup>12</sup> The thermo-



dynamic balance of this process is endoergic by ca. 33 kcal per mol of EDTA.

It should be noted that substitution of EDTA by other electron donors, i.e., cysteine and triethanolamine, similarly results in the photoinduced formation of  $\text{MV}^+$  with the subsequent formation of NADPH. This demonstrates the wide applicability of various electron donors in the system.

In conclusion, we have demonstrated the feasibility of coupling enzymes as catalysts in artificial photosensitized electron-transfer reactions. This approach is useful as a synthetic tool for the light induced preparation of chiral alcohols, as well as a novel attitude for the development of energy conversion and storage systems. It is conceivable that under similar experimental conditions other NADPH-dependent enzymes, i.e., lactate dehydrogenase, glutamic dehydrogenase, and alanine dehydrogenase, would lead to the reduction of other prochiral ketones as well as to the preparation of optically active amino acids.

**Acknowledgment.** The support of the Schonbrunn Fund (Hebrew University) is gratefully acknowledged. This study was performed under the auspices of the Fritz Haber Molecular Dynamics Research Center, The Hebrew University of Jerusalem.

**Registry No.**  $\text{Ru}(\text{bpy})_3^{2+}$ , 15158-62-0;  $(\text{NH}_4)_3\text{EDTA}$ , 15934-01-7;  $\text{MV}^{2+}$ , 4685-14-7;  $\text{NADP}^+$ , 53-59-8; FDR, 9029-33-8; ALDH, 9031-72-5; 2-butanone, 78-93-3; (-)-2-butanol, 14898-79-4.

(12) Willner, I., Ford, W. E.; Otvos, J. W.; Calvin, M. In "Bioelectrochemistry"; Keyzer, H., Gutmann, F., Eds.; Plenum: New York, 1980; pp 55-81.

## Spin Trapping of a Cobalt-Dioxygen Complex

Dorothy E. Hamilton, Russell S. Drago,\* and Joshua Telser

Department of Chemistry, University of Florida  
Gainesville, Florida 32611

Received March 19, 1984

The spin-pairing model for binding  $\text{O}_2$  to transition-metal complexes describes the bound  $\text{O}_2$  as a fragment into which anywhere from 0.1 to 0.8 of an electron is transferred upon binding to the metal.<sup>1-3</sup> As the ligand field strength of the ligands attached to the metal is increased more extensive electron transfer occurs. In all instances the unpaired electron in this system is localized mainly on  $\text{O}_2$  making it difficult to determine the actual charge on this fragment. This charge transfer increases the basicity of a coordinated  $\text{O}_2$  molecule over that of molecular oxygen. For example, it has been shown that trifluoroethanol can hydrogen bond to the terminal oxygen of the  $\text{O}_2$  adduct of [bis(salicylidene- $\gamma$ -iminopropyl)methylamine]cobalt(II) ( $\text{CoSMDPT-O}_2$ ).<sup>4</sup> The magnitude of the shift in the O-H stretching frequency indicates<sup>5</sup> that the enthalpy of hydrogen bond formation is 6.6 kcal mol<sup>-1</sup> making the terminal oxygen of the bound  $\text{O}_2$  about as basic as the carboxyl oxygen in *N,N*-dimethylacetamide.

This work was extended to a study of the Co(II) complex catalyzed oxidation by  $\text{O}_2$  of 2,6-disubstituted phenols to quinones.<sup>6</sup> The mechanism proposed for this reaction<sup>6</sup> suggests that coor-

(1) Tovrog, B. S.; Kitko, D. J.; Drago, R. S. *J. Am. Chem. Soc.* **1976**, *98*, 5144.

(2) Drago, R. S.; Corden, B. B. *Acc. Chem. Res.* **1980**, *13*, 353.

(3) Drago, R. S. In "The Coordination Chemistry of Metalloenzymes"; Drago, R. S., Bertini, I., Luchinat, C., Eds.; Reidel: Dordrecht, Holland, 1983; p 247.

(4) Drago, R. S.; Cannady, J. P.; Leslie, K. A. *J. Am. Chem. Soc.* **1980**, *102*, 6014.

(5) Drago, R. S.; O'Bryan, N.; Vogel, G. C. *J. Am. Chem. Soc.* **1970**, *92*, 3924.

(6) Zombeck, A.; Drago, R. S.; Corden, B. B.; Gaul, J. H. *J. Am. Chem. Soc.* **1981**, *103*, 7580.

(11) Other chemical reductions mediated by viologen radicals have been recently reported; cf.: Goren, Z.; Willner, I. *J. Am. Chem. Soc.* **1983**, *105*, 7764.

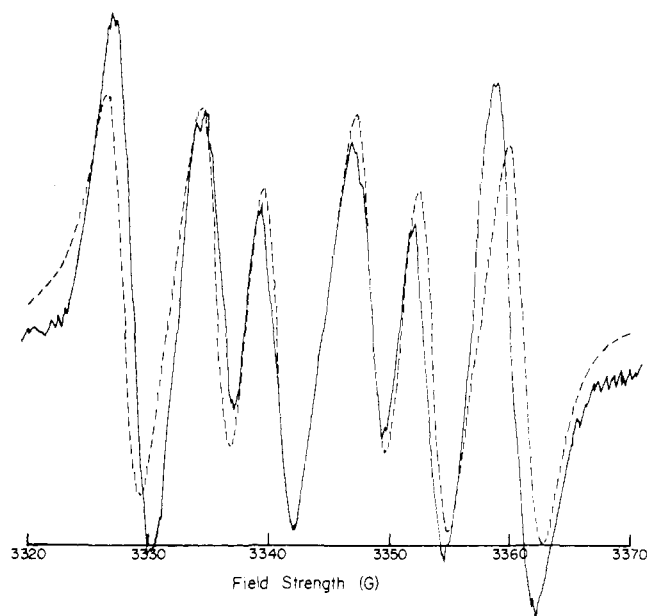
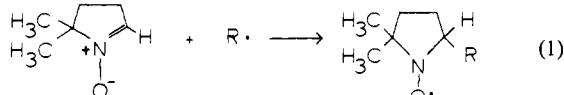


**Figure 1.** Solid line: room temperature EPR spectrum of CoSMDPT-O<sub>2</sub> plus DMPO in toluene. Dashed line: computer simulation of an EPR spectrum with  $g = 2.008$ ,  $A_N = 12.8$  G and  $A_{\beta H} = 7.68$  G.

dination of O<sub>2</sub> to Co(II) not only enhances the basicity of the O<sub>2</sub> but also increases its tendency to undergo free radical reactions. We were thus interested in probing the radical reactivity of Co-O<sub>2</sub> adducts with spin traps.

Spin trapping has been used to aid in the identification of short-lived radicals by EPR spectroscopy. This technique employs a diamagnetic compound which reacts with a free radical to form a relatively stable radical product referred to as a spin adduct.<sup>7,8</sup> This spin adduct is commonly a nitroxide free radical which has a characteristic EPR spectrum. Information about the type of free radical trapped may be obtained from the nitrogen and proton hyperfine coupling constants. The spin trap used in this study is 5,5-dimethyl-1-pyrroline *N*-oxide (DMPO), which functions as a trap as shown in eq 1. The product, a spin adduct of DMPO,



exhibits hyperfine splitting due to both the  $\beta$ -hydrogen and the nitroxide nitrogen. The values are sensitive to the type of radical trapped. DMPO has been used in several studies to trap HO<sub>2</sub> as well as other oxygen-centered radicals.<sup>9-15</sup> Since this spin trap does not form an adduct with free O<sub>2</sub>, reactivity with a metal-bound O<sub>2</sub> would demonstrate enhanced radical reactivity of O<sub>2</sub> as a result of metal coordination.

At room temperature a toluene solution of CoSMDPT that has been exposed to oxygen shows no EPR signal, although at lower temperature (liquid nitrogen) a spectrum for the cobalt-dioxygen complex is observed.<sup>16</sup> When DMPO is added to this CoSMDPT solution an EPR signal at room temperature is immediately observed and is shown in Figure 1. DMPO added to a solution of

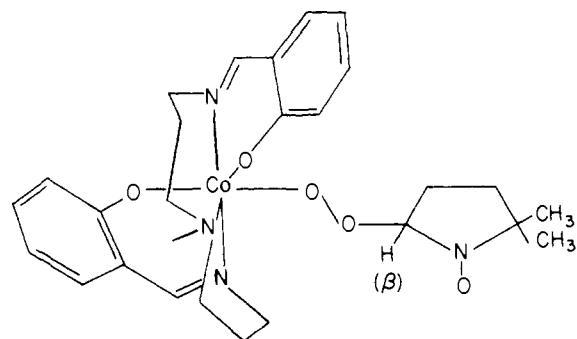


**Figure 2.** Structure of the spin adduct formed by CoSMDPT-O<sub>2</sub> with DMPO.

CoSMDPT prepared in an inert atmosphere does not produce a room temperature EPR spectrum. The CoSMDPT-O<sub>2</sub>/DMPO spectrum is different from that of 5,5-dimethyl-2-pyrroline-1-oxyl (DMPOX), produced by oxidation of DMPO using PbO<sub>2</sub>. This result rules out oxidation of DMPO by CoSMDPT-O<sub>2</sub> as the source of the EPR signal. The EPR spectrum of DMPOX in toluene consists of a triplet with  $g = 2.009$  and  $A_N = 13$  G (37 MHz). Prolonged exposure of the CoSMDPT/DMPO solution to oxygen does lead to formation of DMPOX, since a triplet with  $A_N = 13$  G is seen.

Computer simulation<sup>17</sup> of the EPR spectrum, also shown in Figure 1, leads to a  $g$  value of 2.008 and hyperfine splitting constants as follows:  $A_N = 12.8$  G (36.0 MHz) and  $A_{\beta H} = 7.68$  G (21.6 MHz). The relative magnitudes of the  $A$  values ( $A_N > A_{\beta H}$ ) indicate that an oxygen-centered radical has been trapped.<sup>18,19</sup> The hyperfine splitting values are unlike those for radicals formed when DMPO reacts with either the phenyl ( $A_N = 13.76$ ,  $A_{\beta H} = 19.22$  G) or benzyl radical ( $A_N = 14.16$ ,  $A_{\beta H} = 20.66$  G).<sup>18</sup> This rules out the possibility that radicals arising from reactions of the toluene solvent are being trapped.

We propose that the dioxygen adduct of CoSMDPT, which has one unpaired electron, is trapped by DMPO to yield the spin adduct shown in Figure 2. Since magnetic nuclei more than three bond lengths away from the nitroxide usually do not cause resolvable splitting,<sup>10,18,19</sup> hyperfine splitting due to the cobalt nucleus is not expected.

The superoxide adduct of DMPO in benzene has been reported to have hyperfine splitting values of  $A_N = 12.9$  G and  $A_{\beta H} = 6.9$  G.<sup>13</sup> This reported species may be either the O<sub>2</sub><sup>-</sup> or HO<sub>2</sub> adduct.<sup>10</sup> The values in toluene are expected to be the same because the dielectric constants for the two solvents, which would influence the  $A$  values, are about the same. It is unlikely that the EPR spectrum observed here is that of the superoxide adduct of DMPO. Not only is  $A_{\beta H}$  different, but the generation of free superoxide from CoSMDPT-O<sub>2</sub> is difficult. Walker and co-workers<sup>20</sup> estimated the equilibrium constant for dissociation of CoTPP-O<sub>2</sub> to form superoxide and Co<sup>III</sup>(TPP) to be less than 10<sup>-12</sup>. Furthermore, in a study of the reaction of Co(acacen)py-O<sub>2</sub> with acids, a bimolecular reaction in cobalt was observed and no superoxide detected.<sup>21</sup>

Comparison of the superoxide and Co(SMDPT)-O<sub>2</sub> adduct hyperfine splittings shows that although the  $A_N$  values are about the same (12.9 vs. 12.8 G) there is a significant difference in the  $A_{\beta H}$  values (6.9 G for the superoxide adduct vs. 7.68 G). The  $\beta$ -hydrogen hyperfine coupling depends on the dihedral angle between the C-H <sub>$\beta$</sub>  bond and the nitrogen p orbital.<sup>19</sup> Since the

- (7) Janzen, E. G. *Free Radicals Biol.* **1980**, *4*, 115.  
 (8) Perkins, M. J. *Adv. Phys. Org. Chem.* **1980**, *17*, 1.  
 (9) Harbour, J. R.; Chow, V.; Bolton, J. R. *Can. J. Chem.* **1974**, *52*, 3549.  
 (10) Finkelstein, E.; Rosen, G. M.; Rauckman, E. J. *J. Am. Chem. Soc.* **1980**, *102*, 4994.  
 (11) Finkelstein, E.; Rosen, G. M.; Rauckman, E. J. Paxton, J. *Mol. Pharmacol.* **1979**, *16*, 676.  
 (12) Rosen, G. M.; Rauckman, E. J. *Proc. Natl. Acad. Sci. U.S.A.* **1981**, *78*, 7346.  
 (13) Harbour, J. R.; Hair, L. M. *J. Phys. Chem.* **1978**, *82*, 1397.  
 (14) Harbour, J. R.; Bolton, J. R. *Biochem. Biophys. Res. Commun.* **1975**, *64*, 803.  
 (15) Buettner, G. R.; Oberley, L. W. *Biochem. Biophys. Res. Commun.* **1978**, *83*, 69.  
 (16) Tovrog, B. S.; Drago, R. S. *J. Am. Chem. Soc.* **1974**, *96*, 6765.

- (17) EPR simulations were performed using the program QPOW. See: Belford, R. L.; Nilges, M. J. "Computer Simulation of Powder Spectra", EPR Symposium, 21st Rocky Mountain Conference, Denver, CO; Aug, 1979. Nilges, M. J. Ph.D. Thesis, University of Illinois, Urbana, 1979. Altman, T. E. Ph.D. Thesis, University of Illinois, Urbana, 1981. Maurice, A. M. Ph.D. Thesis, University of Illinois, Urbana, 1982.  
 (18) Janzen, E. G.; Evans, C. A.; Liu, J. I-P. *J. Magn. Reson.* **1973**, *9*, 510.  
 (19) Janzen, E. G.; Evans, C. A.; Liu, J. I-P. *J. Magn. Reson.* **1973**, *9*, 513.  
 (20) Walker, F. A.; Beroiz, D.; Kadish, K. M. *J. Am. Chem. Soc.* **1976**, *98*, 3484.  
 (21) Pignatello, J. J.; Jensen, R. R. *J. Am. Chem. Soc.* **1979**, *101*, 5929.

size of the trapped radical influences this angle, the difference in  $A_{\beta H}$  is probably due to the steric requirements of  $\text{CoSMDPT-O}_2$ . Clearly, we have obtained further support for our earlier conclusions about cobalt(II) coordination enhancing the basicity and reactivity of molecular oxygen.

**Acknowledgment.** We thank the National Science Foundation for financial support of this research. Helpful discussions with Professor Barry B. Corden, Tufts University, are gratefully acknowledged.

**Registry No.**  $\text{CoSMDPT-O}_2$ , 91279-12-8;  $\text{CoSMDPT-O}_2/\text{DMPO}$ , 91210-84-3;  $\text{O}_2$ , 7782-44-7.

### Steric Inhibition of Hyperconjugation. Vanishing Equilibrium Isotope Effect in Bridgehead-Deuterated 2,3-Dimethylbicyclo[2.2.2]octyl Cation

Hans-Ullrich Siehl\* and Harald Walter

*Institut für Organische Chemie, Universität Tübingen  
D-7400 Tübingen, West Germany*

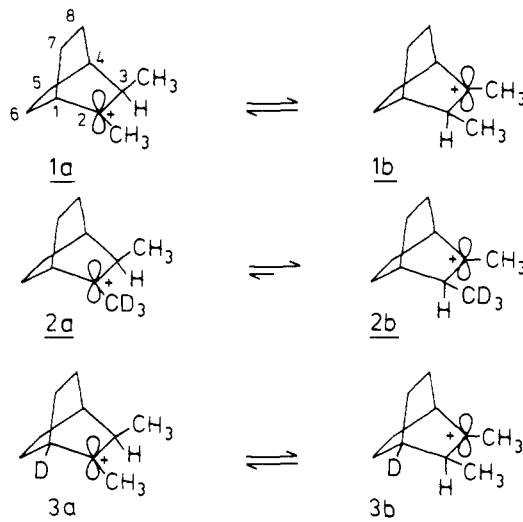
Received March 19, 1984

Secondary isotope effects on reaction rates arise from force-field changes at the isotopic position between the reactant and the transition state.<sup>1</sup> A significant array of experimental results indicate that hyperconjugation makes at least the dominant if not the sole contribution to the  $\beta$ -deuterium isotope effect in carbenium ion solvolysis reactions.<sup>2</sup> Shiner<sup>3</sup> furnished the first data relating the dihedral angle between an adjacent C-H or C-D bond and the vacant p orbital of the cation center with the magnitude of the isotope effect. The magnitude of kinetic isotope effects in solvolysis may be distorted by possible multiple reaction pathways like competing elimination, participation, ion pairing, rearrangements, and other factors.<sup>4</sup> Equilibrium isotope effects in degenerate rearrangements of stable carbocations involve only the properties of well-defined species that can be measured by NMR spectroscopy.<sup>5</sup>

We have investigated the angular dependence of the  $\beta$ -deuterium equilibrium isotope effect in a stable model cation with fixed stereochemistry to prove the hyperconjugational origin unambiguously.

The 2,3-bicyclo[2.2.2]octyl cation **1** combines both prerequisites, a fast degenerate 2,3-hydride shift  $\mathbf{1a} \rightleftharpoons \mathbf{1b}$ , which might be perturbed by  $\beta$ -deuterium, and a fixed dihedral angle of  $90^\circ$  between the vacant p orbital of the cation center and the C-D bond in the bridgehead-deuterated cation **3**. The methyl-deuterated cation **2**, which should show a conformation-independent isotope effect,<sup>6</sup> can serve as a model for the other limiting conformation with a dihedral angle of  $0^\circ$ .

Solutions of **1** in  $\text{SO}_2\text{ClF}/\text{SO}_2\text{F}_2$  were prepared from the corresponding chloride<sup>7</sup> by reaction with  $\text{SbF}_5$  using standard methods.<sup>8</sup> At  $-122^\circ\text{C}$  the  $^{13}\text{C}$  NMR spectrum of **1** (Figure 1a)<sup>9</sup>



shows four peaks (56.12 ppm averaged bridgehead carbons  $\text{C}_1$ ,  $\text{C}_4$ ; 29.43 ppm averaged methylene carbons  $\text{C}_7$ ,  $\text{C}_8$  endo to  $\text{CH}_3$ ; 24.98 ppm averaged methyl carbons; 23.78 ppm averaged methylene carbons  $\text{C}_5$ ,  $\text{C}_6$  exo to  $\text{CH}_3$ ). The peak of the averaged cation and methine carbons  $\text{C}_2$  and  $\text{C}_3$  is not observable due to very large kinetic line broadening at these conditions. Assignments were made from different temperature-dependent line broadening and  $^1\text{H}$ -coupled and  $^1\text{H}$ -specific-decoupled  $^{13}\text{C}$  NMR spectra and were confirmed by analysis of the  $^{13}\text{C}$  NMR spectra of the deuterated cations **2** and **3**. The time-averaged symmetry in the spectrum proves the fast 2,3-hydride shift in cation  $\mathbf{1a} \rightleftharpoons \mathbf{1b}$ . The energy barrier for the 2,3-hydride shift was determined as  $\Delta G^\ddagger = 4.7 \pm 0.15 \text{ kcal/mol}^{10}$  at  $-122^\circ\text{C}$ .

Cation **2** was prepared analogously to **1** from 2-chloro-2-(trideuteriomethyl)-3-methylbicyclo[2.2.2]octane.<sup>7</sup> The  $^{13}\text{C}$  NMR spectrum (Figure 1b) shows typical splittings of the averaged peaks due to the lifting of the degeneracy of the equilibrium  $\mathbf{1a} \rightleftharpoons \mathbf{1b}$ . As expected the largest isotope splittings are observed for those signals showing the largest kinetic line broadening. At  $-122^\circ\text{C}$  the bridgehead-carbon signals are split into two peaks by 6.6 ppm, the  $\text{C}_7$ ,  $\text{C}_8$  carbons by 4.4 ppm, and the  $\text{C}_5$ ,  $\text{C}_6$  carbons by 0.3 ppm. The isotope splitting of the  $\text{CH}_3/\text{CD}_3$  groups is 6.4 ppm. The upfield peak is of lower intensity because of extra broadening due to unresolved deuterium coupling, longer relaxation time, and unfavorable NOE. The upfield shift of the  $\text{CD}_3$  peak is 0.9 ppm larger than the downfield shift of the  $\text{CH}_3$  peak. This shows the direction of the isotope effect. The  $\text{CD}_3$  peak at higher field means the isomeric cation with the  $\text{CD}_3$  group further removed from the positive charge, i.e., **2b**, is favored in the equilibrium  $\mathbf{2a} \rightleftharpoons \mathbf{2b}$ .

Hyperconjugative stabilization of the positive charge decreases the force constants of the C-H bonds in the adjacent methyl group. The zero point energy of this methyl group is lower than that at the remote position. A  $\text{CH}_3$  group has a priori a higher zero point energy than a  $\text{CD}_3$  group, thus  $\text{CH}_3$  is lowered more in energy when attached adjacent to the charged carbon, hence the equilibrium  $\mathbf{2a} \rightleftharpoons \mathbf{2b}$  is shifted toward **2b**. The size of the equilibrium constant is calculated from the isotope splitting. Using the equation<sup>5</sup>  $K = (\Delta + \delta)/(\Delta - \delta)$  we obtain  $K_{\text{CD}_3} = 1.73$  at  $-120^\circ\text{C}$ .

Equilibrium isotope effects and thus the isotope splittings  $\delta$  are temperature dependent.<sup>2</sup> In  $K$  was found to vary linearly with  $1/T$  in the temperature region studied ( $-137$  to  $-92^\circ\text{C}$ ). The thermodynamic parameters for the equilibrium  $\mathbf{2a} \rightleftharpoons \mathbf{2b}$  were determined from  $\ln K = -\Delta H/(RT) + (\Delta S/R)$  via regression analysis as  $\Delta H = 65 \pm 2.5 \text{ cal/mol per D}$  and  $\Delta S = 0.06 \pm 0.007$

(1) Wolfsberg, M.; Stern, M. J. *Pure Appl. Chem.* **1964**, *8*, 325.

(2) Collins, C. J.; Bowman, N. S. Eds. "Isotope Effects in Chemical Reactions"; van Nostrand Reinhold: New York, 1970.

(3) (a) Shiner, V. J., Jr. *J. Am. Chem. Soc.* **1960**, *82*, 265. (b) Shiner, V. J., Jr.; Humphrey, J. S., Jr. *Ibid.* **1963**, *85*, 2416.

(4) See, for example: Shiner, V. J., Jr.; Neumann, T. E.; Fischer, R. D. *J. Am. Chem. Soc.* **1982**, *104*, 354.

(5) (a) Saunders, M.; Vogel, P. J. *J. Am. Chem. Soc.* **1971**, *93*, 2259 and 2561. (b) Saunders, M.; Telkowsky, L. A.; Kates, M. R. *J. Am. Chem. Soc.* **1977**, *99*, 8070.

(6) Sunko, D. E.; Szele, I.; Hehre, W. J. *J. Am. Chem. Soc.* **1977**, *99*, 5000.

(7) Synthetic procedures will be reported in a full paper.

(8) Saunders, M.; Cox, D.; Lloyd, J. R. *J. Am. Chem. Soc.* **1979**, *101*, 6656.

(9) Cations **1-3** are in equilibrium with two isomeric dimethylbicyclo[3.2.1]octyl cations at higher temperatures. Details will be reported in a full paper.

(10) Chemical-shift differences  $\Delta$  for a static cation **1a** were estimated by using 2-methylbicyclo[2.2.2]octyl cation<sup>11</sup> as a model compound.

(11) Kirchen, R. P.; Sorensen, T. S. *J. Am. Chem. Soc.* **1978**, *100*, 1487.

(12) Saunders, M.; Kates, M. R. *J. Am. Chem. Soc.* **1977**, *99*, 8071.